

## The role of circRNA polyribonucleotide nucleoside transferase 1 on gestational diabetes mellitus

Xiaolu Chen<sup>1\*</sup>, Jiaou Huang<sup>1</sup>, Yangying Peng<sup>1</sup>, Yu Han<sup>1</sup>, Xiaoyan Wang<sup>1</sup>, Chuanfa Tu<sup>2</sup>

<sup>1</sup>Department of Obstetrics and Gynecology, Taizhou First People's Hospital, Taizhou 318020, Zhejiang Province, China

<sup>2</sup>Department of Endocrinology and Metabolism, Taizhou First People's Hospital, Taizhou 318020, Zhejiang Province, China

### ARTICLE INFO

#### Original paper

#### Article history:

Received: December 14, 2021

Accepted: April 07, 2022

Published: June 30, 2022

#### Keywords:

*circ-PNPT1; miR-889-3p; PAK1; Gestational diabetes mellitus.*

### ABSTRACT

This study aimed to focus on the mechanism of circRNA polyribonucleotide nucleoside transferase 1 (circ-PNPT1)-mediated miR-889-3p/PAK1 on gestational diabetes mellitus (GDM). Placental tissues from normal pregnancy and GDM patients were collected to detect the levels of circ-PNPT1, miR-889-3p, and PAK1. The high glucose-induced human trophoblast cells HTR-8/SVneo were adopted to stimulate the GDM model in vitro (HG group) and were transfected with lentivirus to silence circ-PNPT1 (si-circ-PNPT1 group) and mimic to overexpress miR-889-3p (miR-889-3p group). Cell proliferation, apoptosis, migration, and invasion were detected by CKK-8, flow cytometry, Transwell, and scratch assay, respectively. The results showed that the expressions of circ-PNPT1 and PAK1 in the GDM patients were up-regulated, and miR-889-3p was down-regulated ( $P < 0.05$ ). Compared with cells in the control group, the circ-PNPT1 and PAK1 in the HG group were up-regulated, and miR-889-3p was down-regulated ( $P < 0.05$ ). The cell proliferation, migration, and invasion abilities were weakened, and the apoptosis rate increased ( $P < 0.05$ ). E-cadherin protein was elevated, and the N-cadherin and Vimentin decreased ( $P < 0.05$ ). Compared with the HG group, the expressions of circ-PNPT1 and PAK1 in the other two groups decreased, and miR-889-3p increased ( $P < 0.05$ ). The cell proliferation, migration, and invasion were enhanced, and the apoptosis rate decreased ( $P < 0.05$ ). E-cadherin, N-cadherin, and Vimentin decreased ( $P < 0.05$ ). There were targeted binding sites for miR-889-3p with circ-PNPT1 and PAK1, indicating circ-PNPT1 promoted HG-induced trophoblast dysfunction through the miR-889-3p/PAK1 axis.

Doi: <http://dx.doi.org/10.14715/cmb/2022.68.6.24>

Copyright: © 2022 by the C.M.B. Association. All rights reserved.

### Introduction

Gestational diabetes mellitus (GDM) is a very common clinical complication of abnormal glucose metabolism during pregnancy. The disease can cause adverse pregnancy outcomes such as miscarriage, fetal growth restriction, neonatal respiratory distress syndrome, and eclampsia (1). In recent years, studies have confirmed that the incidence of GDM in China is increasing year by year, with an incidence of about 11.9%, which has seriously threatened the life and health of mothers and babies (2). The clinical treatment methods for GDM are mainly oral hypoglycemic drugs, diet control, and strengthening exercise, etc., but the treatment effect is not very satisfactory (3). The placenta is an important channel for the exchange of nutrients between the mother and the fetus during pregnancy. Trophoblasts are an important part of the placenta. The invasion and adhesion of trophoblastic cells in the endometrium are important prerequisites for placenta formation (4). Studies have confirmed that abnormal placental function is closely related to GDM-related adverse pregnancy outcomes (5, 6). Therefore, the normal biological function of trophoblast cells in the placenta is of great significance to the development of the placenta.

More and more studies have confirmed that non-coding

ribose nucleic acids (RNAs) play an important role in the regulation of trophoblast function and are closely related to GDM (7, 8). Circular RNAs (circRNAs) are a special class of non-coding RNA molecules, which have a closed-loop structure and are not affected by RNA exonuclease. Compared with other non-coding RNAs, its expression is more stable and not easily degraded. Recent studies have shown that circRNAs have miRNA binding sites and play the role of miRNA adsorption sponges, thereby releasing the inhibitory effect of miRNAs on their target genes and increasing the expression level of target genes. The abnormal expression of circRNA is also involved in the pathological state of some diseases (9). Altesha *et al.* (10) sorted out the significance of circRNA occurrence, characteristics, expression profile, and function to the pathology of heart-related diseases, such as ischemia-reperfusion injury, myocardial infarction, and atherosclerosis. Li *et al.* (11) confirmed that circRNA000203 inhibited the expression of miR-26b-5p and miR-140-3p, and then upregulated the expression of Gata4, exacerbating cardiac hypertrophy. Circ polyribonucleotide nucleoside transferase 1 (circ-PNPT1) is a novel functional circRNA derived from the PNPT1 gene. Wu *et al.* (12) confirmed that circ-PNPT1 was highly expressed in placental tissue and umbilical cord blood of GDM patients. Therefore, it is believed that

\* Corresponding author. Email: [chenxiaolu2022@yandex.com](mailto:chenxiaolu2022@yandex.com)

circ-PNPT1 is involved in regulating the occurrence and development of GDM, but the specific mechanism of action is still unclear.

In this work, the differences in the expression levels of circ-PNPT1, miR-889-3p, and PAK1 in the placental tissues of GDM patients were firstly detected. Secondly, the high glucose-induced trophoblast cells were used to simulate the in vitro GDM model, and the effects of regulating the expression of circ-PNPT1 and miR-889-3p on the biological functions of cell proliferation, apoptosis, migration, and invasion were analyzed. The objective of this work was to provide experimental evidence for understanding the pathogenesis of GDM and finding its therapeutic targets.

## Materials and Methods

### Experimental materials

The human trophoblast cell line HTR-8/SVneo was purchased from ATCC, USA. RPMI-1640 medium, fetal bovine serum, and penicillin-streptomycin dual antibody were purchased from Gibco, USA. Lipofectamine 2000, Annexin V-FITC/PI apoptosis detection kit, lentiviral vector, pGLO vector, and the dual-luciferase reporter gene detection kit were purchased from ThermoFisher, USA. CCK-8 cell proliferation detection kit, E-cadherin, N-cadherin, Vimentin, and PAK1 and GAPDH protein primary and secondary antibodies were purchased from Abcam, UK. cDNA reverse transcription kit and real-time fluorescence quantitative PCR detection kit were purchased from Takara Company in Japan.

### Collection of placenta samples

A total of 40 puerperae who underwent routine obstetric examination and gave birth in Taizhou First People's Hospital from January 2020 to June 2021 were selected as the research subjects, including 20 normal healthy puerperae (normal group) and 20 GDM puerperae (GDM group). Inclusion criteria were set as follows: all singleton births and the pregnancy was terminated by cesarean section after anesthesia; GDM women met the diagnostic criteria established by the World Health Organization in 2013; those who had never received anticoagulants, glucocorticoids, diuretics, and other drug treatments; and those who were aware of the content of this trial and signed the informed consent. Exclusion criteria were given as follows: premature birth or multiple pregnancy; pregnant women with thyroid disease, gestational hypertension, preeclampsia, pregnancy complications, and other medical diseases; and those with congenital heart disease or prenatal fever. This experiment was approved by the Medical Ethics Committee of our hospital, and all subjects signed the informed consent.

After the placenta of the research subjects was delivered, the tissue was collected from the root of the umbilical cord on the central maternal plane of the placenta, avoiding blood vessels and calcifications. The tissue was washed with 0.9% sodium chloride solution and stored at  $-80^{\circ}\text{C}$  for later use.

### Grouping and transfection

HTR-8/SVneo cells were cultured in RPMI-1640 medium containing 10% fetal bovine serum (FBS) and 1% penicillin-streptomycin in a 5%  $\text{CO}_2$  and  $37^{\circ}\text{C}$  constant

temperature incubator. The cells were passaged when they adhered to the wall and the confluence reached about 80%, and they were divided into six groups according to the different test methods. Control group: HTR-8/SVneo cells cultured in conventional conditions without any other treatment. High glucose group (HG group): HTR-8/SVneo cells were cultured with 25 mmol/l glucose medium to prepare an in vitro gestational diabetes cell model. Silencing circ-PNPT1 group (si-circ-PNPT1 group): the circ-PTPN1 lentiviral vector was constructed and transfected into HTR-8/SVneo cells cultured in a high glucose environment. Lentiviral negative control (si-NC): the lentiviral negative control vector of circ-PTPN1 was constructed and transfected into HTR-8/SVneo cells cultured in a high glucose environment. miR-889-3p mimic group (miR-889-3p group): miR-889-3p mimic was synthesized and co-cultured with HTR-8/SVneo cells under high glucose environment. miR-889-3p negative control (miR-NC): the miR-889-3p inhibitor negative control was transfected into HTR-8/SVneo cells cultured in a high glucose environment. The transfection test of HTR-8/SVneo cells was performed using Lipofectamine 2000 reagent.

### CCK-8 to detect the cell proliferation

HTR-8/SVneo cells were seeded into 96-well plates at a concentration of  $3 \times 10^3$  cells/well, and grouped. Then, according to the instructions of the CCK-8 kit, 100  $\mu\text{L}$  of medium containing CCK-8 reagent was added to each well, and incubated at  $37^{\circ}\text{C}$  for 2 hours. Subsequently, the optical density (OD) of each well was detected at a wavelength of 450 nm by a microplate reader, and the proliferation activity of the cells was calculated.

### Flow cytometry to detect apoptosis

Apoptotic and necrotic HTR-8/SVneo cells were stained with Annexin V-FITC/PI apoptosis detection kit. After transfection, it should be trypsinized and centrifuged, and then resuspended in binding buffer for 10 min. 5  $\mu\text{L}$  Annexin V-FITC reagent was added and mixed well. After that, it can add 5  $\mu\text{L}$  PI staining solution, and incubate in an ice bath for 10 min. The flow cytometer was set to the excitation wavelength of 488 nm and the emission wavelength of 530 nm to detect cell apoptosis. Annexin V can stain early apoptotic cell membranes green, and PI can stain late apoptotic or necrotic nuclei red through cell membranes.

### Scratch test to detect cell migration

The HTR-8/SVneo cells in each group were seeded in a 6-well plate at a concentration of  $1 \times 10^6$  cells/well, and a pipette tip can be taken to scratch gently the cells when the cell confluence reached about 80%. The separated cells were rinsed with phosphate buffer, and the cells were routinely cultured for 48 h. The scratch width at 0 h and 48 h was observed with a microscope. The cell migration rate was calculated by cell migration rate = (scratch width 0 hours - scratch width 48 hours)  $\times$  100%, and each experiment was repeated 3 times.

### Transwell chamber assay to detect cell invasion

The diluted Matrigel matrigel was spread on the upper surface of the bottom membrane of the Transwell chamber and incubated until the matrigel was completely confluent. Subsequently, the transfected HTR-8/SVneo cells in each

group were collected, and the cell concentration was adjusted to  $5 \times 10^5$  cells/ml using a serum-free medium. 100  $\mu$ L of cell suspension was added to the upper chamber of the Transwell chamber, and 600  $\mu$ L of the conventional medium was added to the lower chamber to culture for 48 hours. The remaining cells in the upper layer were wiped off with a sterile cotton swab, washed with PBS, fixed with 4% paraformaldehyde for 20 min, and stained with 0.1% crystal violet staining solution for 10 min. Cells were washed with PBS, and the staining of cells in the field of view was observed with a microscope, counted, and averaged.

### Real-time quantitative polymerase chain reaction (RT-qPCR)

Placental tissues of patients in the control group and GDM group were shredded, and total RNA was extracted by the Trizol method and reverse transcribed into cDNA. The expression levels of circ-PNPT1, miR-889-3p, and PAK1 in tissues were detected according to the instructions of the RT-qPCR kit, and U6 or GAPDH was used as the internal reference gene. The total RNA of HTR-8/SVneo cells in each group was extracted by the Trizol method and reversed to cDNA. The expression levels of circ-PNPT1, miR-889-3p, and PAK1 were detected according to the instructions of the RT-qPCR kit, and U6 or GAPDH was used as the internal reference gene. The reaction program was set as follows: pre-denaturation at 94°C for 6 min, denaturation at 94°C for 30s, and annealing at 60°C for 30s (38 cycles). The primer information for quantitative detection of target genes was shown in Table 1, and the relative expression levels of circ-PNPT1, miR-889-3p and PAK1 were detected by using the  $2^{-\Delta\Delta Ct}$  method.

### Western blot detection

The treated cells were taken, and the protein lysis buffer RIPA was added to extract the protein from the HTR-8/SVneo cells, and the quantitative detection of the protein concentration was carried out according to the instructions of the BCA kit. After the sample protein was mixed with the loading buffer, it was boiled and denatured for 5 min. The separating gel and stacking gel of the corresponding concentration were prepared to perform the sodium dodecyl sulfate-polyacrylamide gel electrophoresis (SDS-PAGE) electrophoresis. After electrophoresis, the protein was transferred to Polyvinylidene Fluoride (PVDF) membrane by wet transfer method, placed in a blocking solution containing 5% nonfat milk powder, and blocked for 2 hours at room temperature. After the membrane was rinsed with Tris Buffered Saline Tween (TBST), the diluted primary antibodies E-cadherin, N-cadherin, Vimentin, PAK1,

and GAPDH were added and incubated overnight at 4°C. After the membrane was again rinsed with TBST, diluted HRP-labeled IgG secondary antibody was added and incubated at room temperature for 1 hour. The development of the target protein band was carried out according to the instructions of the electrochemical luminescence (ECL) detection kit, and the gray value of the target protein band was detected and analyzed under the gel imaging system. Using GAPDH as the internal reference gene, the relative expression levels of other genes and proteins were calculated.

### Dual-luciferase reporter gene to detect the target relationship

The relationships between circ-PNPT1 and miR-889-3p, and between miR-889-3p and PAK1 targets were detected using dual-luciferase reporter genes. miR-889-3p and the non-coding regions of circ-PNPT1 and PAK1 containing binding sites/mutation sites were amplified and cloned into pGLO vector to obtain circ-PNPT1 wild type (WT-circ-PNPT1), circ-PNPT1 -PNPT1 mutant (MUT-circ-PNPT1), PAK1 wild type (WT-PAK1), and PAK1 mutant (MUT-PAK1) vectors. HTR-8/SVneo cells in the logarithmic growth phase were taken and seeded in 6-well plates. When the cell confluency reached about 80%, Lipofectamine 2000 reagent was used to perform the transient transfections of miR-NC+WT-circ-PNPT1, miR-889-3p+WT-circ-PNPT1, miR-NC+MUT-circ-PNPT1, miR-889-3p+MUT-circ-PNPT1, miR-NC+WT-PAK1, miR-889-3p+WT-PAK1, miR-NC+MUT-PAK1, and miR-889-3p+MUT-PAK1. After 48 hours, the luciferase activity in each group of cells was detected according to the instructions of the dual-luciferase reporter gene detection kit.

### Statistical methods

Statistical analysis of experimental data was performed using SPSS 19.0 statistical software. The experimental data were expressed as mean  $\pm$  standard deviation (mean  $\pm$  sd), the independent samples t test was used for comparison between two groups, and the one-way ANOVA process was used for comparison between multiple groups, when  $P < 0.05$ , the difference was considered to be statistically significant.

### Results

#### Detected expression levels of circ-PNPT1, miR-889-3p, and PAK1 in the placenta of GDM patients

RT-qPCR detected the differences in the expression levels of circ-PNPT1, miR-889-3p, and PAK1 in placental tissues of normal pregnancy and GDM pregnancy pa-

Table 1. RT-qPCR primer information.

Gene	Primer sequence (5'→3')
circ-PNPT1	F: AGCATGTTAGGCAATGTTGAT R: TTTACTGACCGCTGTGACCA
miR-889-3p	F: GCGCGTTAATATCGGACAAC R: AGTGCAGGGTCCGAGGTATT F: GTCCCTTTGGGTTCGCTGTA
PAK1	R: CCAGTGACCACAAAACGACTAT
U6	F: AAAGCAAATCATCGGACGACC R: GTACAACACATTGTTTCCTCGGA
GAPDH	F: TGTGGGCATCAATGGATTTGG R: ACACCATGTATTCCGGGTCAAT

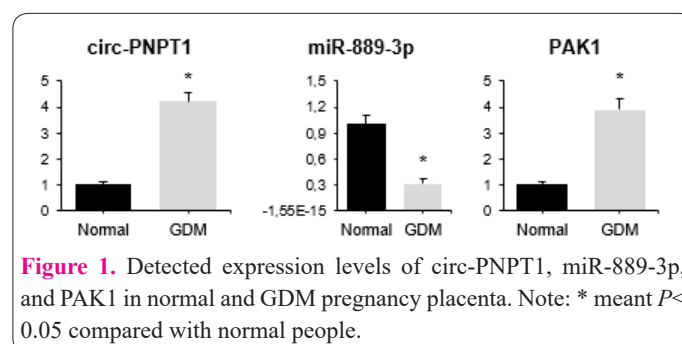


Figure 1. Detected expression levels of circ-PNPT1, miR-889-3p, and PAK1 in normal and GDM pregnancy placenta. Note: \* meant  $P < 0.05$  compared with normal people.

tients, and the results were shown in Figure 1. Compared with normal people, the expression levels of circ-PNPT1 and PAK1 in the placental tissue of GDM patients were significantly increased, while the expression level of miR-889-3p was significantly decreased ( $P < 0.05$ ).

### Detected expression levels of circ-PNPT1, miR-889-3p, and PAK1 in trophoblast cells in each group

RT-qPCR detected the differences in the expression levels of circ-PNPT1, miR-889-3p, and PAK1 in trophoblast cells HTR-8/SVneo in each group, and the results were shown in Figure 2. Compared with the control group, the expression levels of circ-PNPT1 and PAK1 in the cells of the HG group, miR-NC group, and si-NC group were significantly increased, while the expression level of miR-889-3p was significantly decreased ( $P < 0.05$ ). Compared with the HG group, miR-NC group, and si-NC group, the expression levels of circ-PNPT1 and PAK1 in the miR-889-3p group and si-circ-PNPT1 group were significantly decreased, while the expression level of miR-889-3p was significantly increased ( $P < 0.05$ ). There was no significant difference in the expression levels of circ-PNPT1, miR-889-3p, and PAK1 in the cells of the HG group, miR-NC group, and si-NC group ( $P > 0.05$ ). There was no significant difference in the expression levels of circ-PNPT1, miR-889-3p, and PAK1 between the miR-889-3p group and the si-circ-PNPT1 group ( $P > 0.05$ ).

### Effects of circ-PTPN1 and miR-889-3p expression on the proliferation of trophoblast cells

CCK-8 detected the differences between the proliferation rates of trophoblast cells HTR-8/SVneo in each group, and the results were shown in Figure 3. Compared with the control group, the cell proliferation rates in the HG group, miR-NC group, and si-NC group were significantly decreased ( $P < 0.05$ ). Compared with the HG group, miR-NC group, and si-NC group, the cell proliferation rate of the miR-889-3p group and the si-circ-PNPT1 group was significantly increased ( $P < 0.05$ ). There was no significant difference in cell proliferation rate among the HG group, miR-NC group, and si-NC group ( $P > 0.05$ ). There was no significant difference in cell proliferation rate between the miR-889-3p group and the si-circ-PNPT1 group ( $P > 0.05$ ).

### Effects of circ-PTPN1 and miR-889-3p expression on apoptosis of trophoblast cells

Flow cytometry was used to detect the differences in the apoptosis rates of trophoblast HTR-8/SVneo cells in each group, and the results were shown in Figure 4. Compared with the control group, the apoptosis rates of the HG group, miR-NC group, and si-NC group were significantly increased ( $P < 0.05$ ). Compared with the HG group, miR-NC group, and si-NC group, the apoptosis rates of the miR-889-3p group and si-circ-PNPT1 group were significantly decreased ( $P < 0.05$ ). There was no significant difference in the apoptosis rate of the HG group, miR-NC group, and si-NC group ( $P > 0.05$ ). There was no significant difference in apoptosis rate between the miR-889-3p group and the si-circ-PNPT1 group ( $P > 0.05$ ).

### Effects of circ-PTPN1 and miR-889-3p expression on the migration and invasion of trophoblast cells

The Transwell chamber test detected the differences in the number of trophoblast HTR-8/SVneo migration and

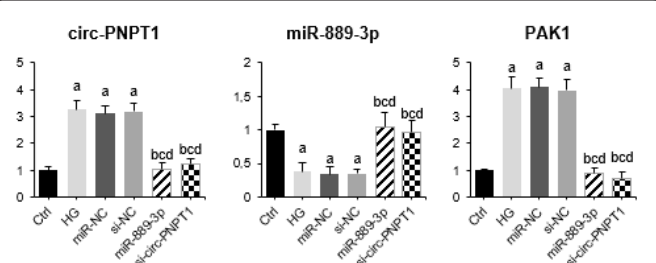


**Figure 2.** Detected expression levels of circ-PNPT1, miR-889-3p, and PAK1 in trophoblast cells HTR-8/SVneo. Note: a, b, c, and d in the figure meant  $P < 0.05$  in contrast to the control group, HG group, miR-NC group, and si-NC group, respectively.

### Cell proliferation (%)

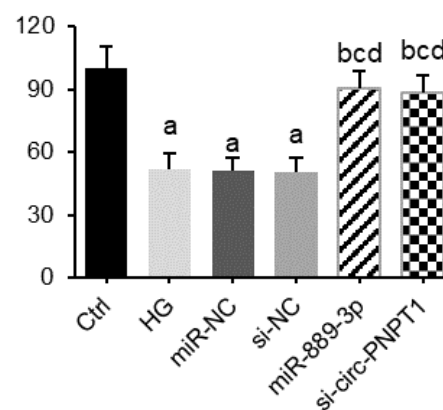


**Figure 3.** Detection of the proliferation rate of trophoblast cells HTR-8/SVneo. Note: a, b, c, and d in the figure meant  $P < 0.05$  in contrast to the control group, HG group, miR-NC group, and si-NC group, respectively.

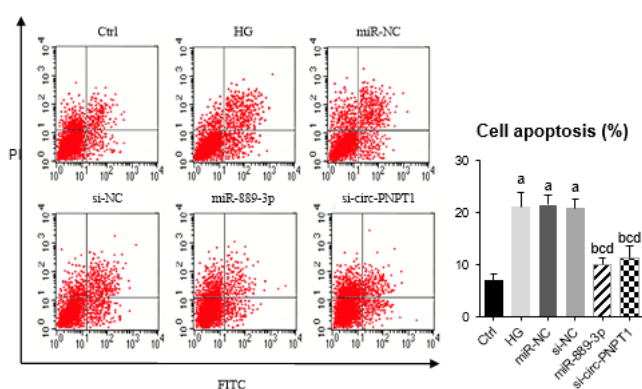


**Figure 4.** Detection of apoptosis rate of trophoblast cells HTR-8/SVneo. Note: a, b, c, and d in the figure meant  $P < 0.05$  in contrast to the control group, HG group, miR-NC group, and si-NC group, respectively.

invasion cells in each group, and the results were shown in Figure 5. Compared with the control group, the numbers of migrating and invasive transmembrane cells in the HG group, miR-NC group, and si-NC group were significantly decreased ( $P < 0.05$ ). Compared with the HG group, miR-NC group, and si-NC group, the numbers of migrating and invasive transmembrane cells in the miR-889-3p group and si-circ-PNPT1 group were significantly increased ( $P < 0.05$ ). There was no significant difference in the number of

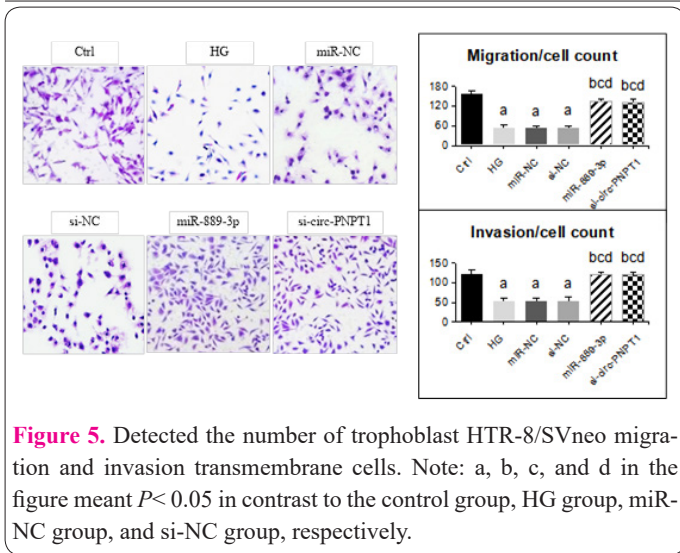


**Figure 5.** Detected the number of trophoblast HTR-8/SVneo migration and invasion transmembrane cells. Note: a, b, c, and d in the figure meant  $P < 0.05$  in contrast to the control group, HG group, miR-NC group, and si-NC group, respectively.

migrating and invasive transmembrane cells among the HG group, miR-NC group, and si-NC group ( $P > 0.05$ ). There was no significant difference in the number of migrating and invasive transmembrane cells between the miR-889-3p group and the si-circ-PNPT1 group ( $P > 0.05$ ).

A Scratch test was used to detect the difference between the healing of trophoblast HTR-8/SVneo in each group, and the results were shown in Figure 6. Compared with the Ctrl group, the wound healing of cells in the HG group, miR-NC group, and si-NC groups was significantly decreased ( $P < 0.05$ ). Compared with the HG group, miR-NC group, and si-NC group, the wound healing of the miR-889-3p group and si-circ-PNPT1 group was significantly increased ( $P < 0.05$ ). There was no significant difference in wound healing among the HG group, miR-NC group, and si-NC group ( $P > 0.05$ ). There was no significant difference in wound healing between the miR-889-3p group and the si-circ-PNPT1 group ( $P > 0.05$ ).

**Effects of circ-PTPN1 and miR-889-3p expression on the expressions of PAK1, E-cadherin, N-cadherin, and Vimentin in trophoblast cells**

Western blot was adopted to detect the differences in the protein expression levels of PAK1, E-cadherin, N-

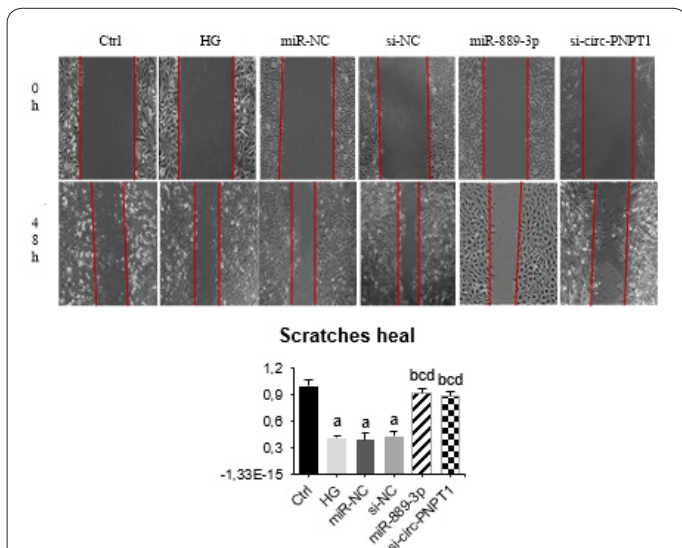


**Figure 6.** Scratch healing assay of trophoblast HTR-8/SVneo. Note: a, b, c, and d in the figure meant  $P < 0.05$  in contrast to the control group, HG group, miR-NC group, and si-NC group, respectively.

cadherin, and Vimentin in trophoblast cells HTR-8/SVneo in each group. The results were shown in Figure 7. Compared with the control group, the protein expressions of PAK1 and E-cadherin in the cells of the HG group, miR-NC group, and si-NC groups were significantly increased, while the protein expressions of N-cadherin and Vimentin were significantly decreased ( $P < 0.05$ ). Compared with the HG group, miR-NC group, and si-NC group, the protein expression levels of PAK1 and E-cadherin in the miR-889-3p group and the si-circ-PNPT1 group were significantly decreased, while the protein expression levels of N-cadherin and Vimentin were significantly increased ( $P < 0.05$ ). There was no significant difference in the expression levels of PAK1, E-cadherin, N-cadherin, and Vimentin in the HG group, miR-NC group, and si-NC group ( $P > 0.05$ ). There was no significant difference in the protein expression levels of PAK1, E-cadherin, N-cadherin, and Vimentin between the miR-889-3p group and the si-circ-PNPT1 group ( $P > 0.05$ ).

**Verification of the targeting relationship of circ-PTPN1, miR-889-3p, and PAK1**

The binding targets of circ-PTPN1 and miR-889-3p, PAK1 and miR-889-3p were predicted, and the targeting relationship between the two was detected by the dual luciferase reporter gene. The results were shown in Figure 8. After co-transfection of WT-circ-PNPT1 and miR-889-3p, the relative activity of dual-luciferase was significantly decreased after co-transfection of WT-PAK1 and miR-889-3p ( $P < 0.05$ ).

**Discussion**

GDM is a disorder of abnormal glucose metabolism during pregnancy, which is likely to cause adverse pregnancy outcomes such as fetal growth restriction (13). Placental tissue is an important tissue for the exchange of

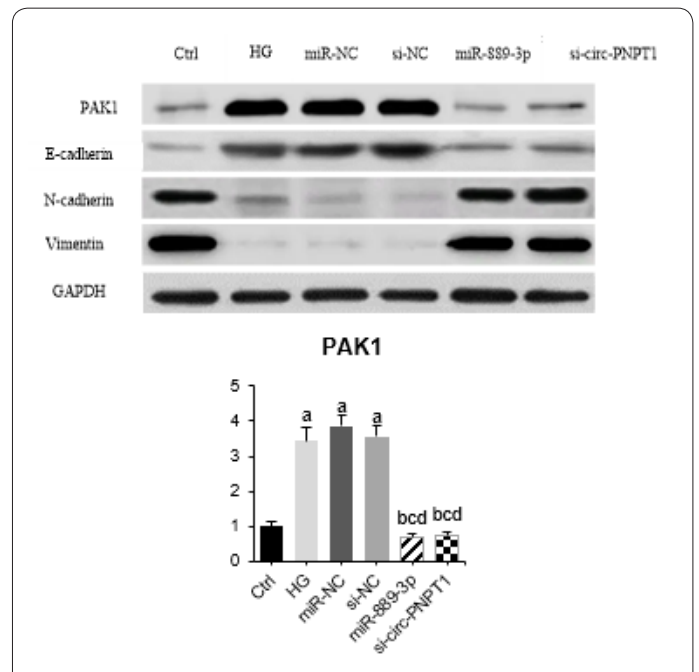
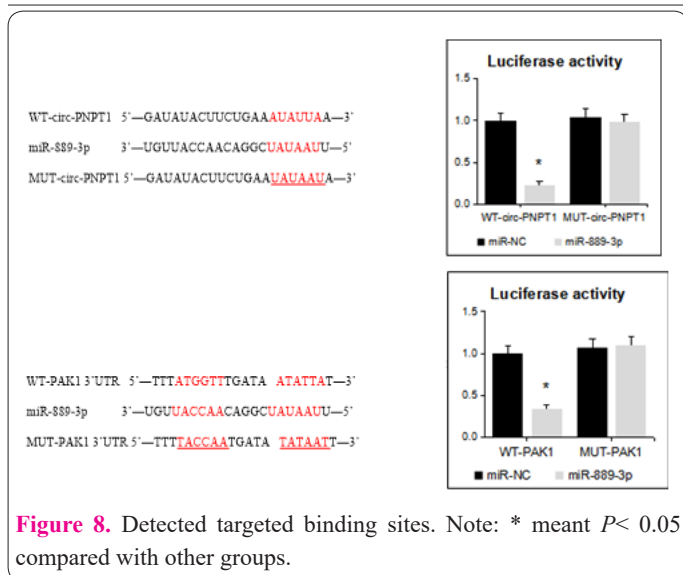


**Figure 7.** Western blot detection of target protein expression level of HTR-8/SVneo in trophoblast cells. Note: a, b, c, and d in the figure meant  $P < 0.05$  in contrast to the control group, HG group, miR-NC group, and si-NC group, respectively.



nutrients between mother and fetus during pregnancy, and trophoblast cells are an important part of placental tissue (14, 15). The migration and invasion of trophoblast cells are normal physiological phenomena, which can fix the placenta and the fetus. At present, a large number of studies have confirmed that there are abnormal expressions of genes in the placental tissue of GDM patients. These genes can regulate the function of placental trophoblast cells, hinder the normal function of the placenta, and then participate in the process of GDM (16, 17). Both circRNA and miRNA are non-coding RNA molecules. miRNA can target the post-transcriptional level of mRNA to regulate its expression level, while circRNA can adsorb miRNA and play a role in regulating mRNA expression (18). CircRNAs and miRNAs are involved in regulating the progression of GDM and other diseases. Yu *et al.* (19) showed that the expression level of miR-96-5p in the placenta and plasma of GDM patients was reduced, and overexpression of miR-96-5p under high glucose conditions could promote the proliferation of trophoblast cells. Chen *et al.* (20) confirmed that the expression of circ0001173 was down-regulated in the plasma of GDM patients, while the expression of circ0008285 was up-regulated. In addition, knocking down the expression of circ0008285 in a high-glucose environment could inhibit the proliferation, invasion, and migration of HTR-8/SVneo cells. In this work, it was found that the expression level of circ-PNPT1 was up-regulated in placental tissue of GDM patients and in HTR-8/SVneo cells induced by high glucose. High glucose-induced HTR-8/SVneo cells can inhibit cell proliferation, migration, and invasion, and promote apoptosis. Such results are consistent with the results of Peng *et al.* (21) and Wu *et al.* (22). Inhibition of circ-PNPT1 expression can reverse the high glucose-induced inhibition of proliferation, migration, and invasion of HTR-8/SVneo cells, and promote the apoptosis. It indicated that circ-PNPT1 is involved in the GDM process, and knockdown of circ-PNPT1 expression could protect the function of GDM trophoblast cells.

There are abnormally expressed miRNAs in the placenta of GDM patients, and miRNAs can also affect the normal function of the placenta by regulating the function of trophoblast cells (23). Zhao *et al.* (24) confirmed that the expression of miR-221 was down-regulated in the placental tissue of GDM rats, and it can target and bind to

PAK1 to regulate the proliferation, apoptosis, and insulin secretion of pancreatic  $\beta$  cells. Li *et al.* (25) showed that the expression of miR-96 was down-regulated in the placental tissue of GDM patients, which can target the collective PAK1 to regulate insulin secretion and  $\beta$ -cell function. The results of this work found that the expression level of miR-889-3p was decreased, while the expression of PAK1 was increased in placental tissue of GDM patients and high glucose-induced HTR-8/SVneo cells. Overexpression of miR-889-3p also reversed the inhibition of proliferation, migration, and invasion of HTR-8/SVneo cells induced by high glucose, and the promotion of apoptosis. Therefore, it is speculated that miR-889-3p can target the PAK1 gene to play a role in the function of trophoblast cells.

E-cadherin is an epithelial marker, while N-cadherin and Vimentin are mesenchymal markers (26, 27). The expression of E-cadherin protein was increased in HTR-8/SVneo cells induced by high glucose, while the protein expressions of N-cadherin and Vimentin were decreased. Inhibiting the expression of circ-PNPT1 or increasing the expression of miR-889-3p could reverse the protein expression changes of E-cadherin, N-cadherin, and Vimentin. These results indicate that circ-PNPT1 and miR-889-3p can promote the epithelial-mesenchymal transition of trophoblast cells, which in turn increases the ability of trophoblast cells to migrate and invade. Finally, this work verified the target relationship between miR-889-3p and circ-PNPT1, miR-889-3p and PAK1 using dual luciferase reporter genes. It indicated that circ-PNPT1 could regulate the miR-889-3p/PAK1 axis to play a regulatory role in trophoblast cell dysfunction in GDM.

Circ-PNPT1 can target miR-889-3p and then regulate the expression of PAK1, play a role in inhibiting the proliferation, migration, and invasion of GDM trophoblast cells, and promote the apoptosis of trophoblast cells and epithelial-mesenchymal transition. This work only simulated the in vitro model of GDM to analyze the mechanism of circ-PNPT1/miR-889-3p/PAK1 on the biological function of trophoblast cells. In the future, GDM animal models needed to be prepared for further verification of its regulatory function. The results of this work can provide a reference for understanding the process of GDM and finding new therapeutic targets.

## References

### References

1. Lende M, Rijhsinghani A. Gestational diabetes: overview with emphasis on medical management. *Int J Environ Res Public Health* 2020; 17(24): 9573.
2. Juan J, Yang H. Prevalence, prevention, and lifestyle intervention of gestational diabetes mellitus in China. *Int J Environ Res Public Health* 2020; 17(24): 9517.
3. Mack LR, Tomich PG. Gestational diabetes: diagnosis, classification, and clinical care. *Obstet Gynecol Clin* 2017; 44(2): 207-217.
4. Olmos-Ortiz A, Flores-Espinosa P, Díaz L, Velázquez P, Ramírez-Isarraraz C, Zaga-Clavellina V. Immunoendocrine dysregulation during gestational diabetes mellitus: the central role of the placenta. *Int J Mol Sci* 2021; 22(15): 8087.
5. Li Y-x, Long D-l, Liu J et al. Gestational diabetes mellitus in women increased the risk of neonatal infection via inflammation and autophagy in the placenta. *Medicine* 2020; 99(40).

6. Bedell S, Hutson J, de Vrijer B, Eastabrook G. Effects of maternal obesity and gestational diabetes mellitus on the placenta: current knowledge and targets for therapeutic interventions. *Curr Vasc Pharmacol* 2021; 19(2): 176-192.
7. Filardi T, Catanzaro G, Mardente S et al. Non-coding RNA: role in gestational diabetes pathophysiology and complications. *Int J Mol Sci* 2020; 21(11): 4020.
8. Vasu S, Kumano K, Darden CM, Rahman I, Lawrence MC, Naziruddin B. MicroRNA signatures as future biomarkers for diagnosis of diabetes states. *Cells* 2019; 8(12): 1533.
9. Yi Y, Liu Y, Wu W, Wu K, Zhang W. Reconstruction and analysis of circRNA-miRNA-mRNA network in the pathology of cervical cancer. *Oncol Rep* 2019; 41(4): 2209-2225.
10. Altesha MA, Ni T, Khan A, Liu K, Zheng X. Circular RNA in cardiovascular disease. *J Cell Physiol* 2019; 234(5): 5588-5600.
11. Li H, Xu J-D, Fang X-H et al. Circular RNA circRNA\_000203 aggravates cardiac hypertrophy via suppressing miR-26b-5p and miR-140-3p binding to Gata4. *Cardiovasc Res* 2020; 116(7): 1323-1334.
12. Wu H, Wu S, Zhu Y et al. Hsa\_circRNA\_0054633 is highly expressed in gestational diabetes mellitus and closely related to glycosylation index. *Clin Epigenet* 2019; 11(1): 1-13.
13. Lai M, Liu Y, Ronnett GV et al. Amino acid and lipid metabolism in post-gestational diabetes and progression to type 2 diabetes: A metabolic profiling study. *PLoS Med* 2020; 17(5): e1003112.
14. Fisher JJ, Vanderpeet CL, Bartho LA et al. Mitochondrial dysfunction in placental trophoblast cells experiencing gestational diabetes mellitus. *J Physiol* 2021; 599(4): 1291-1305.
15. Guo X, Yin B, Wang C, Huo H, Aziziaram Z. Risk assessment of gastric cancer in the presence of *Helicobacter pylori* cagA and hopQII genes. *Cell Mol Biol* 2021; 67(4): 299-305.
16. Peng H-Y, Li H-P, Li M-Q. Downregulated ABHD5 aggravates insulin resistance of trophoblast cells during gestational diabetes mellitus. *Reprod Sci* 2020; 27(1): 233-245.
17. Lorenzon AR, Moreli JB, de Macedo Melo R et al. Stromal cell-derived factor (SDF) 2 and the endoplasmic reticulum stress response of trophoblast cells in gestational diabetes mellitus and in vitro hyperglycaemic condition. *Curr Vasc Pharmacol* 2021; 19(2): 201-209.
18. Yang Y, Yujiao W, Fang W et al. The roles of miRNA, lncRNA and circRNA in the development of osteoporosis. *Biol Res* 2020; 53(1): 1-16.
19. Yu X, Liu Z, Fang J, Qi H. miR-96-5p: a potential diagnostic marker for gestational diabetes mellitus. *Medicine* 2021; 100(21).
20. Chen H, Zhang S, Wu Y et al. The role of circular RNA circ\_0008285 in gestational diabetes mellitus by regulating the biological functions of trophoblasts. *Biol Res* 2021; 54.
21. Peng HY, Li MQ, Li HP. High glucose suppresses the viability and proliferation of HTR-8/SVneo cells through regulation of the miR-137/PRKAA1/IL-6 axis. *Int J Mol Med* 2018; 42(2): 799-810.
22. Bousfield D. Revisiting cyber-diplomacy: Canada–China relations online. *Globalizations* 2017; 14(6): 1045-1059.
23. Zhu W, Shen Y, Liu J et al. Epigenetic alternations of microRNAs and DNA methylation contribute to gestational diabetes mellitus. *J Cell Mol Med* 2020; 24(23): 13899-13912.
24. Zhao H, Tao S. MiRNA-221 protects islet  $\beta$  cell function in gestational diabetes mellitus by targeting PAK1. *Biochem Biophys Res Commun* 2019; 520(1): 218-224.
25. Li L, Wang S, Li H et al. microRNA-96 protects pancreatic  $\beta$ -cell function by targeting PAK1 in gestational diabetes mellitus. *Biofactors* 2018; 44(6): 539-547.
26. Hong L, Han K, Wu K et al. E-cadherin and ZEB2 modulate trophoblast cell differentiation during placental development in pigs. *Reproduction* 2017; 154(6): 765-775.
27. Liu M, Chen X, Chang Q-X et al. Decidual small extracellular vesicles induce trophoblast invasion by upregulating N-cadherin. *Reproduction* 2020; 159(2): 171-180.